



Two-Time Correlations for Probing the Aging Dynamics of Glassy Colloids

Journal:	<i>Soft Matter</i>
Manuscript ID	SM-ART-10-2018-002191
Article Type:	Paper
Date Submitted by the Author:	26-Oct-2018
Complete List of Authors:	Robe, Dominic; Emory University, Physics Boettcher, Stefan; Emory University, Physics

Cite this: DOI: 10.1039/xxxxxxxxxx

Two-Time Correlations for Probing the Aging Dynamics of Glassy Colloids

Dominic Robe and Stefan Boettcher^aReceived Date
Accepted Date

DOI: 10.1039/xxxxxxxxxx

www.rsc.org/journalname

We present results for the aging dynamics of a dense 2D colloidal system obtained with molecular dynamics simulations. To this end, systems are quenched to densities far above the glass transition with relaxation time scales that used to be prohibitive for such a comprehensive study. We performed extensive simulations to gather detailed statistics about rare rearrangement events. With a simple criterion for identifying irreversible events based on Voronoi tessellations, we find that the rate of those events decelerates hyperbolically. We track the probability density function for particle displacements, the van-Hove function, with sufficient statistics as to reveal its two-time dependence that is indicative of aging. Those displacements, measured from a waiting time t_w after the quench up to times t , exhibit a data collapse as a function of t/t_w . These findings can be explained comprehensively as manifestations of record dynamics, i.e., a relaxation dynamic driven by record-breaking fluctuations. We show that an on-lattice model of a colloid that was built on record dynamics indeed reproduces the experimental results in great detail.

1 Introduction

A rapid quench of a colloid from a liquid state to densities well above the glass transition initiates a far-from-equilibrium relaxation dynamics known as “physical aging”¹ or glassy relaxation. Understanding physical aging carries implications for many fields, from theories of complex systems² to manufacturing of packaging materials.³ Glassy dynamics appear in granular media⁴ and biological systems^{5,6}, and have applications to food handling and drug design.⁷ In aging, observables retain a memory of the waiting time t_w since the quench, signifying the breaking of time-translational invariance and the non-equilibrium nature of the state. For example, measures of the activity within the system taken over some time-window $\Delta t = t - t_w$, such as the van-Hove distribution of particle displacements, are now a function of two time-scales, Δt and t_w , instead of just the lag-time Δt , as would be the case in a steady state. As has been observed previously^{8–11}, those distributions are characterized by broadened, non-Fickian tails that get broader with time Δt , but each in a manner that is characteristic of its age. Those tails clearly emphasize the fact that anomalously large fluctuations in the displacement of particles drive the structural relaxation, which proves intimately related^{12,13} to the spatial dynamic heterogeneity as well as the temporal intermittency that have been observed in many experiments.^{8,11,14–22} The dynamic events of interest are therefore rare

and non-self-averaging, requiring many independent simulations of large systems to yield clear results. Further, examination of both short and long time scales requires both a high temporal resolution and long simulation runs. For these reasons, an experimental study of an aging colloidal system on *two* timescales with sufficient accuracy is a daunting task and has not been attempted yet.

Here we measure the two-time behavior of the fundamental van-Hove distribution of particle displacements during aging, provide a scaling collapse of the data, and comprehensively explain our observations in terms of the preeminence of intermittent events. To this end, we reconstruct the setting of the simplest of such an experiment²⁰, a planar bi-disperse colloid subjected to a rapid volume quench deep into the glassy regime, as a molecular dynamics simulation. In our simulations we first reproduce previously published results of the experiment for mean-square displacements of particles in great detail. Using an equivalent criterion to identify irreversible relaxation events as in Ref.²⁰, we find in particular that the rate of such events declines with age as $\sim 1/t$, shown also for the experimental data recently in Ref.²³. Those results demonstrate that the simulation significantly extends the accuracy of the measurements by using a large number of instances. Then, we present results for the particle displacement distribution, i.e., the van-Hove function, that indeed reveal a dependence on both Δt and t_w , indicative of aging. The distribution of displacements spreads out with increasing Δt , as

^a Department of Physics, Emory University, Atlanta, GA 30322, USA

one would expect in any relaxing system. However, if Δt is fixed but t_w is increased, the distribution narrows, demonstrating the decreasing activity due to structural changes during aging. The data readily collapses as a function of $\Delta t/t_w$ over a wide range of times. By the fundamental nature of the van-Hove function²⁴, this implies similar scaling in many other observables. We finally show that all of these results can be reproduced with a recently proposed lattice model¹³ based on the simple fact that the relaxation dynamics requires ever larger (record-sized) fluctuations in the cluster of activated particles.^{2,12,25}

2 Simulation Details

The simulations of the colloidal system are performed using the Python molecular dynamics package HOOMD-Blue.^{26,27} Each simulation contains 100,000 particles with periodic boundary conditions. The particles form a 50/50 bidisperse mixture with diameter ratio 1.4. Trajectories are computed using Newtonian integration with a harmonic repulsive interaction potential given by $E(r_1, r_2) = \varepsilon(|\mathbf{r}_1 - \mathbf{r}_2| - r_1 - r_2)^2$, where \mathbf{r}_1 and \mathbf{r}_2 are the positions of particles 1 and 2, and r_1 and r_2 are their radii. The simulation temperature and particle interaction strength ε are chosen to make dynamic time and length scales comparable to previous work. In this manner, one simulation “second” corresponds roughly to one second in the experiments of Ref.²⁰. The simulations are run at 74% packing fraction for 5 seconds, which is empirically found to equilibrate the system. Then the simulation box is rapidly compressed in .1 sec to a packing fraction of 84%. We then record particle positions every 10^{-2} sec for 20 sec. This protocol is repeated for 10 independent realizations.

It should be noted that the interaction potential here is deliberately short-range non-attractive to emulate colloidal dynamics. In contrast to the common Lennard-Jones systems, where temperature is the parameter controlling the glass transition, this system more like hard disks. Here the packing fraction is the important control parameter, and the temperature merely serves to set the speeds that particles travel at between collisions. It should also be emphasized that these simulations are carried out deep in the glassy regime, and after the volume quench the systems continue aging for the entire simulation. We see no reason why any other potential, whether short or long-ranged would alter qualitatively the picture we are presenting here. However, any attractive potential could lead to the formation of a gel and follow a different phenomenology.

All particles in our simulations obviously experience many collisions during a simulation, most of which restrain a particle to a local “cage” formed by the tight constraints its neighbors impose on its mobility.⁸ After some time particles might spontaneously undergo a cooperative rearrangement. Such a rearrangement is noticeable in a single particle’s trajectory as a shift to a new position, as seen in Fig. 1. It is noteworthy that the distance traveled to a new cage is usually within the normal range of in-cage rattling displacements, making the distinction between the two types of motion a subtle one. In fact, the difference in a particle’s position before and after a rearrangement can be less than 10% of its diameter and only changes in the neighborhood topology (as detectable by a Voronoi tessellation, for example) may suffice

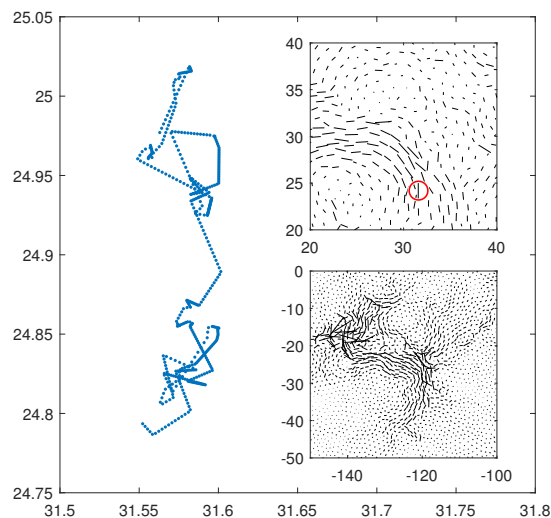


Fig. 1 Example trajectory of a particle. The particle is temporarily confined to an apparent cage, and undergoes a rearrangement to a new cage. Axes are system coordinates in units of small particle diameter. Top inset: Circled line is the net displacement of the drawn trajectory. Similar net displacements are drawn for nearby particles. Bottom inset: a wider view of a larger rearrangement emphasizes the broad distribution of displacement distances. Note the displacements in both insets are scaled up for visibility. Displacements are typically less than a tenth of a particle diameter.

to qualify such a displacement as irreversible (see below). Nevertheless, we argue that these spontaneous rearrangements are the mechanism responsible for aging in glassy systems.

3 Results

Simulation results for the system-averaged mean squared displacement (MSD) starting from different waiting times are shown in Fig. 2(a). MSD is usually considered as a function of waiting time t_w and lag-time $\Delta t = t - t_w$, as shown. The system demonstrates the typical plateau associated with caging, followed by diffusion on longer time scales as cages are escaped. The height of the plateau suggests a caging length scale between about 1% and 10% of a particle diameter. Beyond that, the dynamics is driven by activated events and the particles intermittently move $> 10\%$ of a diameter. These ranges are consistent with the ex-

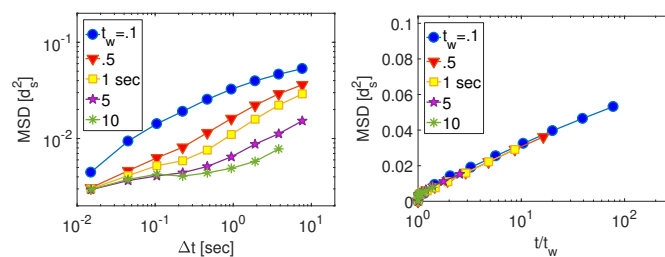


Fig. 2 (a) Mean Squared Displacement (MSD) in units of d_s^2 , where d_s is the diameter of the small particles, plotted as a function of lag-time $\Delta t = t - t_w$, when the MSD is measured starting at age t_w . It shows how a glass stagnates with age. (b) A collapse of the data from (a) shows that the MSD is invariant with respect to t/t_w . These simulation results closely resembles the behavior of the experimental data from Yunker et al²⁰ as shown in Fig. 3 of Ref.²³.

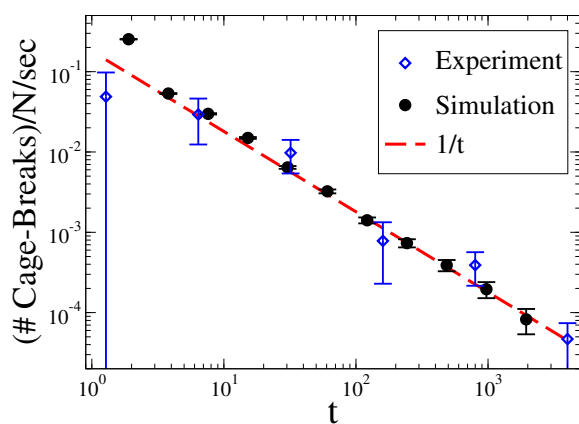


Fig. 3 Decay in the rate of irreversible neighborhood swaps in a jammed colloid in the simulations. Overlaid is the corresponding experimental data for intermittent cage-breaks (“quakes”) from Fig. 2a of Yunker et al²⁰, as previously discussed in Ref.²³. The data is consistent with the hyperbolic decay, $\sim 1/t$ (dashed line), predicted by record dynamics.¹³

perimental trajectories seen in Ref.²⁰. We also see the plateaus getting longer with increased t_w . For very early waiting times, the cages are so short-lived that there is no apparent plateau, but the growing caging time scale is still apparent as a shift in the diffusive part of the curve. It should be noted that the word “diffusive” is used loosely here. If the MSD curves were truncated earlier, then one could mistake the upturn in them for straight lines on a log-log scale, see Fig. 2(a). However, on longer time scales, the curves for the earlier waiting times begin to level off. We do not consider this as the approach to another plateau, but rather indicative of the nature of physical aging. If cooperative rearrangements are due to record-breaking fluctuations, and each rearrangement between t_w and t ratchets up the MSD, then the MSD increases roughly logarithmically with Δt ^{13,23}, as explained via Eq. (2) below. This expectation is verified by Fig. 2(b), which shows the exact same MSD data collapsed when plotted as function of $\log(t/t_w)$.

Measurement of the rate at which cooperative rearrangements occur requires some sort of discretization of the system dynamics. The distribution of particle displacements itself does not easily allow for discrimination between caged and rearranging particles. As we will discuss below that distribution is characterized by a Gaussian core at shorter distances and an exponential tail further out, with merely a gradual transition between them, see Fig. 4. The exponential tail has been attributed to rearranging particles, but may also be due to heterogeneity in cage sizes.²⁸ These facts make rearrangement detection based on particle displacements dubious. However, subtle changes in the configuration can be detected by considering changes among neighboring particles. To that end, the radical Voronoi tessellation is computed for each frame of six simulations using the C++ library Voro++.²⁹ A history is constructed of every pair of particles which are neighbors at any point in the simulation. For each neighbor pair, the first frame of the simulation in which that pair are neighbors is also recorded. In this manner, a particle which never rearranges in the entire simulation would have roughly six “new” neighbors in the

first frame, then none for the rest of the simulation. When a rearrangement occurs, the Voronoi tessellation changes, and a few particles encounter new neighbors. Reversible in-chage fluctuations might create flickering Voronoi networks, but these changes can be shaken out in a few frames by only counting the *first* contact with a neighbor. Not all particles in a rearranging region will make new contacts, and some rearrangements send particles back to old neighbors, but as long as a consistent fraction of rearranging particles encounter new neighbors, a count of the new neighbors in a given frame is a reasonable measure of the rearrangement event rate.

For their particle tracking experiments, Yunker et al²⁰ also defined irreversible neighborhood swaps that were shown to decay with time after the quench. Simply binning their data logarithmically, it was shown in Ref.²³ that the experimental rate of those events decays with age in a manner that is consistent with $\sim 1/t$. Using the Voronoi method described above, we determine the corresponding event rate in the simulations to find a perfect match with that experimental data, see Fig. 3. Moreover, due to the ability to rerun the simulation many times, the decay in the rate appears to be hyperbolic to a high degree of statistical significance.

Going beyond mere comparisons with existing experimental results, we can now use our simulation to study two-time correlations that thus far have proven impossible to access with sufficient accuracy in experiments. For example, in Fig. 4 we show results for the single-axis particle displacement distribution over a time-window Δt starting at t_w ,

$$G_s(\Delta x, t_w, \Delta t) = \sum_i \delta(|x_i(t_w + \Delta t) - x_i(t_w)| - \Delta x), \quad (1)$$

also known as the self-part of the van Hove function.²⁴ In our simulations, for $\Delta t < 10^{-3}$ sec (not shown), few collisions have occurred, so the distribution of displacements would be largely due to the distribution of particle velocities. On intermediate time scales, $\Delta t \approx 10^{-2}$ sec, the distribution is determined by the cage size distribution. On longer time scales, the distribution begins to spread out, as previously observed in similar simulations in Ref.^{10,30}, for example. In Fig. 4(a) for $t_w \approx 1$ sec, this spreading begins at around .1 sec, but the spreading begins later with increasing t_w .

Note that G_s in Fig. 4 exhibits exponential “non-Fickian” tails, beyond the dominant Gaussian fluctuations at short distances, that signify rare intermittent behavior, similar to observations in spin-glass simulations.^{31–33} It has been measured previously in various colloidal experiments and simulations^{8–11,28,34,35}, but averaged over long time intervals that blend together various waiting times t_w . While the shape of G_s is generally invariant, the weight of this tail increases with Δt , but it decreases with age t_w , since activated cage rearrangements become increasingly harder. Amazingly, all data collapses when the time-window Δt is rescaled by the age t_w . Similar to the analysis of the MSD in Fig. 2(b), by scaling the lag time with the waiting time, we should observe the same number of rearrangements for any given $\Delta t/t_w$, if the rearrangements correspond to record breaking fluctuations. In Fig. 4, two collections of curves are plotted accordingly, one set with $\Delta t/t_w = 1$, and another with $\Delta t/t_w = 5$. Note that many com-

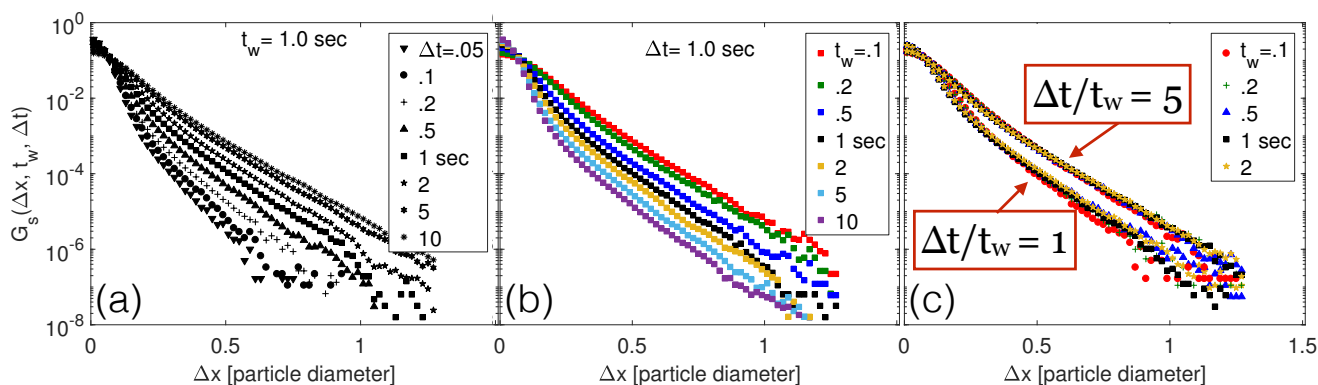


Fig. 4 Distribution of single particle displacements $G_s(\Delta x, t_w, \Delta t)$ in the simulations (self-part of van-Hove function), as defined in Eq. (1). (a) The distribution spreads out *more* with increasing Δt (different symbols) at some fixed waiting time $t_w = 1 \text{ sec}$. (b) The distribution spreads out *less* over a fixed time window Δt with increasing t_w (different colors). (c) These distributions collapse for fixed ratios of $\Delta t/t_w$, as predicted by record dynamics, see Fig. 5. These figures are averages over all particles. Small and large particles behave qualitatively similar.

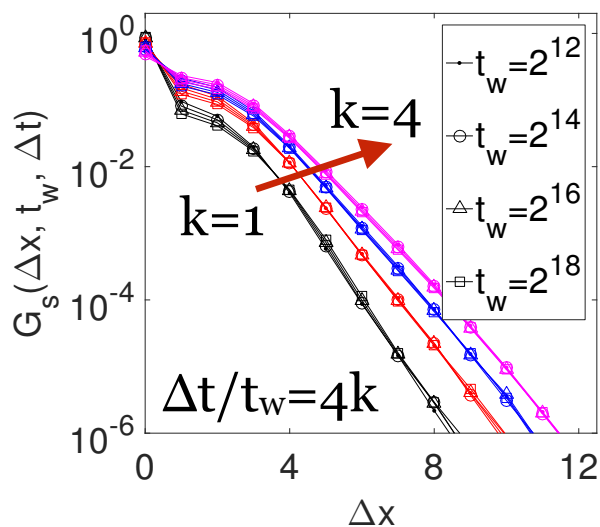


Fig. 5 Plot of the van-Hove particle displacement distribution G_s in Eq. (1) in the cluster model. Note the similarity in the exponentially broadened (non-Fickian) tails compared with the simulation data in Fig. 4. Here, G_s is measured at four different waiting times t_w (different symbols), each over four different time-windows $\Delta t = t - t_w$ (different colors) such that $\Delta t/t_w = 4k$ with $k = 1, \dots, 4$. For each k , the respective data collapses.

mon dynamical observables, such as MSD or the self-intermediate scattering function (and, thus, the persistence^{10,13,23}) can be calculated from the van Hove function.²⁴ In demonstrating the collapse of G_s , we have shown that all measures involving averages over single-particle displacements would collapse similarly. The collapse of these curves suggests that the dynamics of this aging system is driven by record-sized fluctuations: if $\Delta t \ll t_w$, quasi-equilibrium in-cage rattle dominates while rare, intermittent and irreversible cage-breaks encountered for $\Delta t \geq t_w$ drive the actual non-equilibrium relaxation process. As these break-ups require record-sized fluctuations that decelerate with $\sim 1/t$, the statistics is invariant for $\Delta t/t_w$, as the following considerations explain.

4 Conclusions

In the experiment and simulations, anomalously large cage break events are found to substantially relax the system and must be viewed as distinct from the Gaussian fluctuations of in-cage rattle. Yet, such a relaxation must entail a structural change, which makes subsequent relaxations even harder. For example, to facilitate a cage-break, Yunker et al²⁰ observed that a certain number of surrounding particles have to conspire via some rare, random fluctuation. For that event to qualify as irreversible, the resulting structure must have increased stability, however marginal. A following cage-break thus requires even more particles to conspire. With each of those fluctuations exponentially unlikely in the number of participating particles³⁵, cage-breaks represent *records* in an independent sequence of random events that “set the clock” for the activated dynamics. In such a statistic, record events are produced at a *decelerating* rate of $\lambda(t) \propto 1/t$, consistent with the results in Fig. 3. As those records do not cause each other, we obtain a log-Poisson statistics, for which the average number of intermittent events in an interval $t_w < t < t_w + \Delta t$ is

$$\langle n_I(\Delta t, t_w) \rangle \propto \int_{t_w}^{t_w + \Delta t} \lambda(\tau) d\tau \propto \ln(1 + \Delta t/t_w), \quad (2)$$

which explicitly depends on the age t_w . Then, any two-time observable, like the van-Hove distribution in Eq. (1), becomes *subordinate*¹⁹ to this clock: $G_s(\Delta t, t_w) = G_s[n_I] = G_s(\Delta t/t_w)$. In ref-

erence to a Poisson statistic, where a constant rate λ provides time-translational invariance (stationarity) with $\langle n_l \rangle \propto t - t_w$, this record dynamics is a log-Poisson process.³⁶ We have indeed verified the log-Poisson property for our simulations.³⁷ The generality of this argument may address the astounding commonality in slow relaxation that holds across many glassy systems, quenched and structural, irrespective of microscopic details.²³

To verify that record-breaking fluctuations are sufficient to produce the observed dynamics, we also apply our analysis of the van Hove function to a simple coarse grained model. We examine the recently proposed cluster model of aging¹³, which forgoes the simulation of microscopic dynamics, and places particles on a lattice. Each particle belongs to a cluster, and clusters are contiguous, non-overlapping, and space filling. In every update, a cluster of size h has $P(h) \propto e^{-h}$ chance to break into h single-particle clusters. If $h = 1$ already, then the updating particle swaps position with a random neighbor while also joining its cluster. In this manner, when a cluster breaks up, it's neighboring clusters spread rapidly over it's territory in a series of such smaller displace-and-attach events. The number of clusters thereby decreases by one, and the average cluster size increases marginally³⁸, slowing the system dynamics.

Within clusters, fast dynamics ("in-cage rattle"), perceived as leading to the re-arrangements preceding a cluster break, are intentionally coarse-grained out, with their collective effect replaced by $P(h)$. As shown in Ref.¹³, cluster-breaking events indeed decelerate as $\sim 1/t$, comparable to Fig. 3, and follow the log-Poisson process in Eq. (2). With particles re-mobilizing only when activated by a cluster break, their mean-squared displacement (MSD) grows indeed logarithmically with time, similar to Fig. 2, i.e., proportional to the accumulated number of those events in Eq. (2). Following the definition in Eq. (1), we have measured G_s also for displacements of particles in the cluster model. Fig. 5 shows that this data reproduces the $\Delta t/t_w$ -collapse for the van Hove distribution of particle displacements found in the molecular dynamics simulations. Note that the Gaussian peak at zero displacement in the MD simulation data in Fig. 4 is replaced with a delta function since the cluster model coarse-grains out the in-cage rattle.

In summary, we have shown that the logarithmic slowdown of dynamics in an aging glass can be credited to the behavior of record-breaking fluctuations. We expected the system dynamics to be controlled by rearrangement events, which should happen on a schedule set by the statistics of new records. We found that the event rate decays as $1/t$, and that the entire distribution of single-particle dynamics seems to be subordinate to this same schedule. It should be noted again that any system-averaged dynamic observation such as mean squared displacement or intermediate scattering function can be calculated from this distribution, so this is a far-reaching result. Clearly for these events to have this effect there must be some associated structural change, but we do not claim a particular structure metric or rearrangement pathway, merely that whatever rearrangement does occur makes the next one more difficult. This alone seems sufficient to describe the dynamics of an aging glass. This generality is important because different glass-forming systems may operate by

different microscopic mechanisms, but the phenomenology of aging can still be shared.

In future simulations, we intend to analyze the effect on aging of varying the density attained after a quench. As in the experiments, we expect that those variations (above a certain threshold of about 81%) will merely affect some pre-factors numerically without changing the log-Poisson characteristic of the aging.²³ The corresponding variation in the cluster model is achieved by varying the exponential in $P(h)$, which affects each observable there. Finding a response to such variation that is equivalent for *all* observables between cluster model and molecular dynamics simulation provides a substantial test for the record dynamics interpretation.

Conflicts of Interest

There are no conflicts to declare.

Acknowledgements

We thank Paolo Sibani and Eric Weeks for many enlightening discussions, and Justin Burton for computational resources.

Notes and references

- 1 L. Struik, *Physical aging in Amorphous polymers and other materials* (Elsevier Science Ltd, New York, 1978).
- 2 P. Anderson, H. J. Jensen, L. P. Oliveira, and P. Sibani, *Complexity* **10**, 8 (2004).
- 3 C. Arnoldmckenna and G. Mckenna, *J. Res. Natl. Inst. Stand. Technol.* **98**, 523 (1993).
- 4 B. Kou, Y. Cao, J. Li, C. Xia, Z. Li, H. Dong, A. Zhang, J. Zhang, W. Kob, and Y. Wang, *Nature* **551**, 360 (2017).
- 5 D. Bi, J. H. Lopez, J. M. Schwarz, and M. L. Manning, *Nat. Phys.* **11**, 1074 (2015).
- 6 S. Hengherr, M. R. Worland, A. Reuner, F. Brümmer, and R. O. Schill, *Physiol. Biochem. Zool.* **82**, 749 (2009).
- 7 G. G. Kenning, 2014 IEEE Int. Conf. RFID, IEEE RFID 2014, 134 (2014).
- 8 E. R. Weeks, J. C. Crocker, A. C. Levitt, A. Schofield, and D. a. Weitz, *Science* (80-.). **287**, 627 (2000).
- 9 P. Chaudhuri, L. Berthier, and W. Kob, *Phys. Rev. Lett.* **99**, 2 (2007).
- 10 D. El Masri, L. Berthier, and L. Cipelletti, *Phys. Rev. E - Stat. Nonlinear, Soft Matter Phys.* **82**, 1 (2010).
- 11 T. Kajiya, T. Narita, V. Schmitt, F. Lequeux, and L. Talini, *Soft Matter* **9**, 11129 (2013).
- 12 S. Boettcher and P. Sibani, *J. Phys. Condens. Matter* **23**, 065103 (2011).
- 13 N. Becker, P. Sibani, S. Boettcher, and S. Vivek, *J. Phys. Condens. Matter* **26**, 7 (2014).
- 14 L. Buisson, L. Bellon, and S. Ciliberto, *J. Phys. Condens. Matter* **15**, S1163 (2003).
- 15 L. Buisson, S. Ciliberto, and A. Garcimartín, *Europhys. Lett.* **63**, 603 (2003).
- 16 H. Bissig, S. Romer, L. Cipelletti, V. Trappe, and P. Schurtenberger, *PhysChemComm* **6**, 21 (2003).

- 17 G. F. Rodriguez, G. G. Kenning, and R. Orbach, *Phys. Rev. Lett.* **91**, 1 (2003).
- 18 L. Oliveira, H. Jensen, M. Nicodemi, and P. Sibani, *Phys. Rev. B* **71**, 1 (2005).
- 19 P. Sibani, G. F. Rodriguez, and G. G. Kenning, *Phys. Rev. B - Condens. Matter Mater. Phys.* **74**, 1 (2006).
- 20 P. Yunker, Z. Zhang, K. B. Aptowicz, and a. G. Yodh, *Phys. Rev. Lett.* **103**, 1 (2009).
- 21 R. Candelier, O. Dauchot, and G. Biroli, *Phys. Rev. Lett.* **102**, 1 (2009).
- 22 T. Yanagishima, J. Russo, and H. Tanaka, *Nat. Commun.* **8**, 1 (2017).
- 23 D. M. Robe, S. Boettcher, P. Sibani, and P. Yunker, *Epl* **116**, 1 (2016).
- 24 K. Binder and W. Kob, *Glassy Materials and Disordered Solids* (World Scientific, 2011).
- 25 P. Sibani and P. B. Littlewood, *Phys. Rev. Lett.* **71**, 1482 (1993).
- 26 J. A. Anderson, C. D. Lorenz, and A. Travasset, *J. Comput. Phys.* **227**, 5342 (2008).
- 27 J. Glaser, T. D. Nguyen, J. A. Anderson, P. Lui, F. Spiga, J. A. Millan, D. C. Morse, and S. C. Glotzer, *Comput. Phys. Commun.* **192**, 97 (2015).
- 28 R. Colin, A. M. Alsayed, J.-C. Castaing, R. Goyal, L. Hough, and B. Abou, *Soft Matter* **7**, 4504 (2011).
- 29 C. H. Rycroft, *Chaos* **19** (2009), 10.1063/1.3215722.
- 30 A. J. Archer, P. Hopkins, and M. Schmidt, *Phys. Rev. E* **75**, 040501 (2007).
- 31 A. Crisanti and F. Ritort, *Europhys. Lett.* **66**, 253 (2004).
- 32 P. Sibani and H. J. Jensen, *Europhys. Lett.* **69**, 563 (2005).
- 33 P. Sibani, *Phys. Rev. E - Stat. Nonlinear, Soft Matter Phys.* **74**, 1 (2006).
- 34 D. a. Stariolo and G. Fabricius, *J. Chem. Phys.* **125**, 064505 (2006).
- 35 E. R. Nowak, J. B. Knight, E. Ben-Naim, H. M. Jaeger, and S. R. Nagel, *Phys. Rev. E* **57**, 1971 (1998).
- 36 P. Sibani and H. J. Jensen, *Stochastic dynamics of complex systems: from glasses to evolution (series on complexity science)* (Imperial College Press, 2013).
- 37 S. Boettcher, D. Robe, and P. Sibani, Unpublished .
- 38 C. Tang, K. Wiesenfeld, P. Bak, S. Coppersmith, and P. Littlewood, *Phys. Rev. Lett.* **58**, 1161 (1987).